ADVANCED FUNCTIONAL MATERIALS
www.afm-journal.de

The Relationship of Solid-State Plasticity to Mechanochromic Luminescence in Difluoroboron Avobenzone Polymorphs

Gamidi Rama Krishna, Mangalampalli S. R. N. Kiran, Cassandra L. Fraser, Upadrasta Ramamurty, and Chilla Malla Reddy**

In solid-state mechanochromic luminescence (ML) materials, it remains a challenge to establish the origin of fluorescence color changes upon mechanical action and to determine why only some fluorophores exhibit ML behavior. The study of mechanical properties by nanoindentation, followed by ML experiments on green- and cyan-emitting polymorphs of difluoroboron avobenzone reveals that upon smearing, the plastically deformable cyan form shows a prominent color change to yellow, while in the harder green form the redshifted emission is barely detectable. Crystal structure analysis reveals the presence of slip planes in the softer cyan form that can facilitate the formation of recoverable and low energy defects in the structure. Hence, the cyan form exhibits prominent and reversible ML behavior. This suggests a potential design strategy for efficient ML materials.

1. Introduction

Organic solid-state emitters are of great interest due to their promising applications as light-emitting diodes,[1] lasers,[2] two-photon fluorescent materials[3] and opto-electronic devices.[4] It is important to understand the structure-property correlations in these materials in order to tune and control the luminescence. Emission colour changes can be effected by perturbing the structure, as fluorescence strongly depends on the molecular structure, conformation and intermolecular interactions, both in solution and solid states. For example, it has been reported that the ordered aggregates of $[(C_6F_5Au)_2(\mu\text{-}1,4\text{-diisocyanobenzene})]$ emit yellow; whereas, the amorphous form luminesces blue.[5] Yoon et al.[4] reported two-colour reversible fluorescence switching in response to pressure, temperature and solvent vapour in the solid-state of a cyanodistyrylbenzene derivative. They have attributed this to the two-directional shear-sliding ability of molecular sheets in its blue and green emitting phases. Recently, Jones and co-workers showed tuning of fluorescence in a stilbene-based organic materials by changing the crystal structure via co-crystal formation with halogenated compounds.[6] Fraser et al.[7] examined the multiple emissive aggregation states of difluoroboron avobenzone (BF_2AVB) to show that they emit green, cyan and blue colours under UV light depending on the intermolecular interactions (**Figure 1**). Additionally, the BF_2AVB crystals were shown to exhibit a reversible colour change on mechanical crushing or smearing, which is known as mechanochromic luminescence (ML). The origin for the reversible ML behavior in this system is yet to be established. Moreover in solid state ML materials, it has long been a challenge to establish 1) whether the fluorescence color changes originate from the aggregates or from conformers of a single molecule and 2) why only some fluorophores exhibit the ML behavior.

Previous studies suggest a strong correlation between the ML behavior and structure of organic crystals. However, precise quantification of mechanical properties of ML materials, the objective of this study, has not been performed. This is necessary if structure-mechanochromic luminescence relationships are to be understood. Here, this is accomplished by nanoindentation,

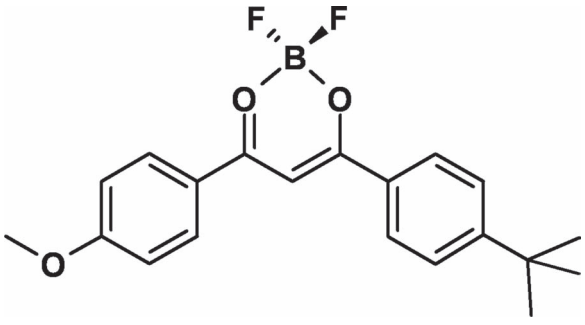

Figure 1. Chemical structure of difluoroboron avobenzone, BF_2AVB.

G. R. Krishna, Prof. C. M. Reddy
Department of Chemical Sciences
Indian Institute of Science Education and Research
Kolkata, 741252, West Bengal, India
E-mail: cmreddy@iiserkol.ac.in
Dr. M. S. R. N. Kiran, Prof. U. Ramamurty
Department of Materials Engineering
Indian Institute of Science
Bangalore, 560012, India
E-mail: ramu@materials.iisc.ernet.in
Prof. C. L. Fraser
Department of Chemistry
University of Virginia
Charlottesville, VA 22904, USA

DOI: 10.1002/adfm.201201896

which allows for the measurement of elastic modulus, *E*, and hardness, *H*, on relatively small crystals of BF_2AVB. The nanoindentation technique has proven useful in quantifying the mechanical behavior of different solid forms to establish structure-mechanical property correlation in molecular crystals and organic-inorganic frameworks,[8] particularly in cases where the other conventional techniques, such as X-ray crystallography, fail. For example, Varughese et al. have identified the spatial distribution of inter-grown domains of two structurally similar aspirin polymorphs in the crystals, which could not be confirmed by single crystal X-ray crystallography.[9] Here in this study, we examined two of the three known polymorphic forms of BF_2AVB by both qualitative and quantitative mechanical tests: 1) mechanical deformation using a metal forceps and a needle and 2) nanoindentation, in order to establish relationships between crystal structures, mechanical properties and the reversible mechanochromic luminescence in the solid-state crystals.

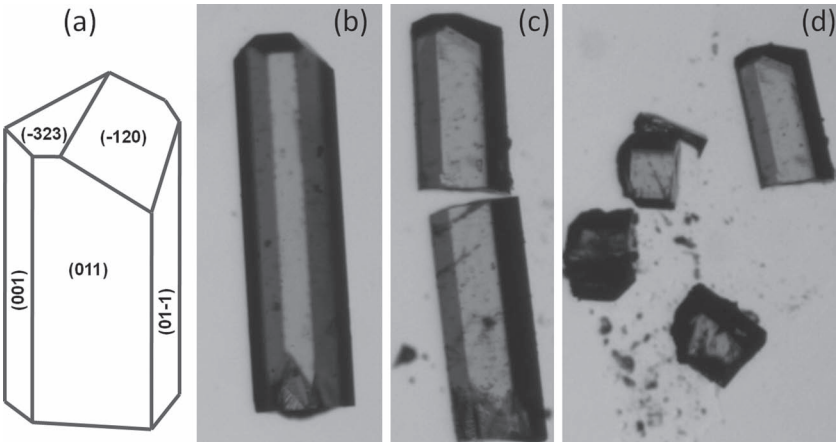

Figure 2. Green polymorph of BF_2AVB (form I). a) Schematic diagram of the habit planes, shown with the face indices. Photographs of b) as-grown crystal and c,d) after application of a mechanical stress. Notice the crystal breakage in (c) and (d).

2. Results and Discussion

BF_2AVB is known to exist in at least three polymorphic forms, each with distinct emission colours under UV black light at 365 nm.[7] We obtained the single crystals with a size that is at least 2 mm^3 (a vital prerequisite for the studies) for green (form **I**) and cyan (form **II**) polymorphs of BF_2AVB from acetone solution, using procedures reported elsewhere.[7] The X-ray crystal structures of these polymorphs are orthorhombic, with space group *Pnma* for green and monoclinic, $P2_1/c$ for cyan emitting solids.[7] The third polymorph (blue emission) grows into a dendritic crystal morphology upon rapid solvent evaporation; hence, a suitable single crystal for nanoindentation could not be obtained. We do not discuss this form further.

2.1. Qualitative Studies: Structural Basis for Brittle and Ductile Properties

Deformation behaviors of forms I and II were first examined by stressing the crystals with a metal forceps and needle while viewing them under a stereo microscope. Form I broke into pieces (**Figure 2**) under test conditions, which implies that it is brittle in nature.[10] In contrast, form II could be bent permanently on the (001) crystal face (**Figure 3**). However, under identical conditions, the perpendicular pair of crystal faces (100) did not show any sign of bending, but broke. Such bending behavior in molecular crystals is not unprecedented. It occurs when the strong and weak intermolecular interactions are arranged in orthogonal directions in crystal packing, for example, hexachlorobenzene and 3,4-dichlorophenol.[10] On the contrary, crystals with nearly isotropic interactions in all directions show brittle behavior.[10c,d] A careful inspection of the crystal packing in the two forms indeed indicates such features.

In form I, BF_2AVB molecules are connected via weak C–H···O hydrogen bonds to form 1D chains (**Figure 4**a) that run parallel to each other in the ac-plane. The *tert*-Bu groups from two adjacent 1D chains pack on the same side, similar to a zipper, leaving the BF_2 groups to cluster on the opposite side.[7] This results in a flat 2D molecular arrangement parallel to the (010) plane. The layers pack one over the other with the adjacent arenes (Ar) offset relative to each other to optimize the π-stacking interactions. As a result, the *tert*-Bu groups from one layer pack on top of the –OMe groups in the next layer. Since the *tert*-Bu groups within a layer are packed similar to that in a zipper, this plane is not expected to be active for slippage. Hence, the (010) plane with the π-stacking interactions is expected to act as the major slip plane in this structure, but the weakness of the intralayer interactions and absence of any

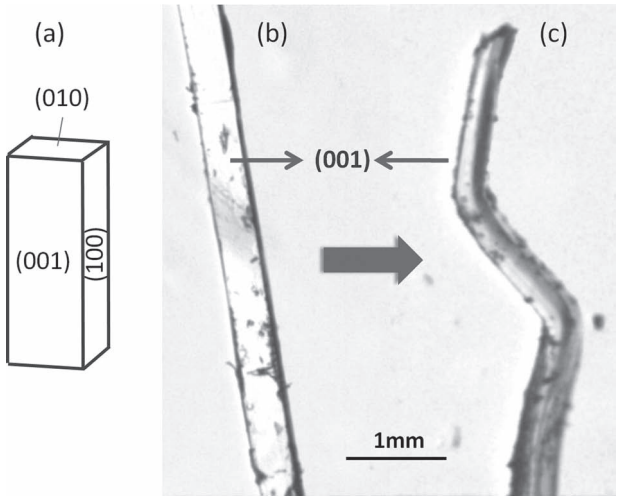

Figure 3. Cyan polymorph of BF_2AVB (form II). a) Schematic of the crystal face indices. Images of b) as-grown crystal and c) after mechanical deformation. Note the bending deformation in crystal (c) along the (001) plane.

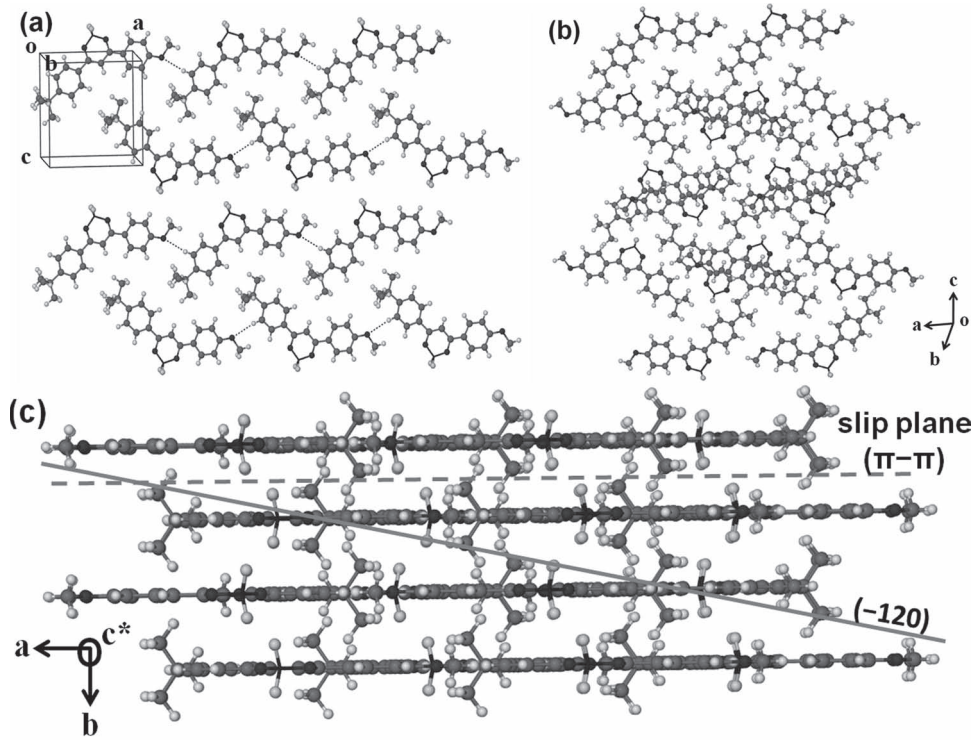

Figure 4. Crystal structure of the BF_2AVB green form I (brittle). a) Top view of a 2D sheet to show 1D tapes formed via C–H···O interactions and the packing of similar groups of molecules on the same side. Crystal packing views perpendicular to b) (011) and c) (001) plane, i.e., side view of 2D sheets. Notice the molecular packing with respect to the indentation directions perpendicular to (011) in (b), and (–120) and (001) planes in (c).

strong interactions along any direction makes the two slip planes energetically comparable. Hence, it is not surprising to find that these crystals are brittle.[10c,d]

In form II, multiple C–H···F interactions (d/Å, θ/°; 2.587 Å, 158.84°; 2.643 Å, 166.01°; 2.427 Å, 137.88°; 2.611 Å, 117.15°) between molecules lead to the formation of thick 2D sheets parallel to the (100) plane (**Figure 5**). In general an individual C–H···F interaction is not considered to be strong but their presence in multiple numbers makes the sheets significantly strong as compared to that in form I where only one C–H···O interaction is present per molecule.[11] From the crystal packing, it is evident that there are two potential slip planes in the structure, one packed with *tert*-Bu groups and the other with –OMe groups, both bonded via only the van der Waals forces (Figure 5a). The plastic bending behavior in the cyan form could be understood from the recently proposed bending model,[10a] according to which the arrangement of weak interactions in one plane coupled with relatively stronger interactions perpendicular to it is necessary for bending in molecular crystals. In the process of crystal bending on the (001) face, the weak interaction planes slip past one another while the relatively stronger interactions in other directions keep the molecular sheets intact.

2.2. Quantitative Studies: Nanoindentation

Nanoindentation experiments were possible on (011), (001) and (–120) facets of I and only on (001) of II. Experiments on the other two faces of form II crystals could not be conducted due to their extremely soft nature. Representative load, P, depth of penetration, h, curves are shown in **Figure 6**. All three plots of form I (green lines) show large residual depths upon unloading, which indicate that the crystal undergoes significant plastic deformation during indentation. The P-h curves obtained from (001), (–120) and (011) of I have several discrete displacement bursts ('pop-ins') in the loading portion indicating that the plastic deformation occurs intermittently. The P-h curve of (011) for I has one most significant pop-in, which repeatedly occurs at $P = 2.6 \pm 0.3$ mN and $h = 4.1 \pm 0.2$ μm with a pop-in magnitude, Δh, of ≈250 nm. In form I, the pop-in intensity is higher for (001) and the first pop-in occurs at a lower load than those in the other two faces. This indicates that the onset of plasticity is significantly easier in (001). While the smaller pop-ins have Δh of ≈10 nm, it is ~ 30 nm for bigger pop-ins and they appear to occur alternately. Notably, these Δh (10 and 30 nm) are integral multiples (6 and 17 times) of crystal lattice ($c = 1.73$ nm) on the (001) face, which is consistent with our earlier reports on other organic crystals.[8,9] On the (–120) face, the P-h curve is relatively smooth compared to the other two faces but it exhibits a pop-in signature with very small Δh. The P-h curve of (001) for form II shows (Figure 6) that both the pop-in intensity and the penetration depth are higher than any face of I, highlighting the much softer nature of form II. The residual impression of indent on the (001) face for II shows significant pile-up along the two edges on the indenter (figure not shown) whereas no pile-up was found for the major face, (011) of I. The

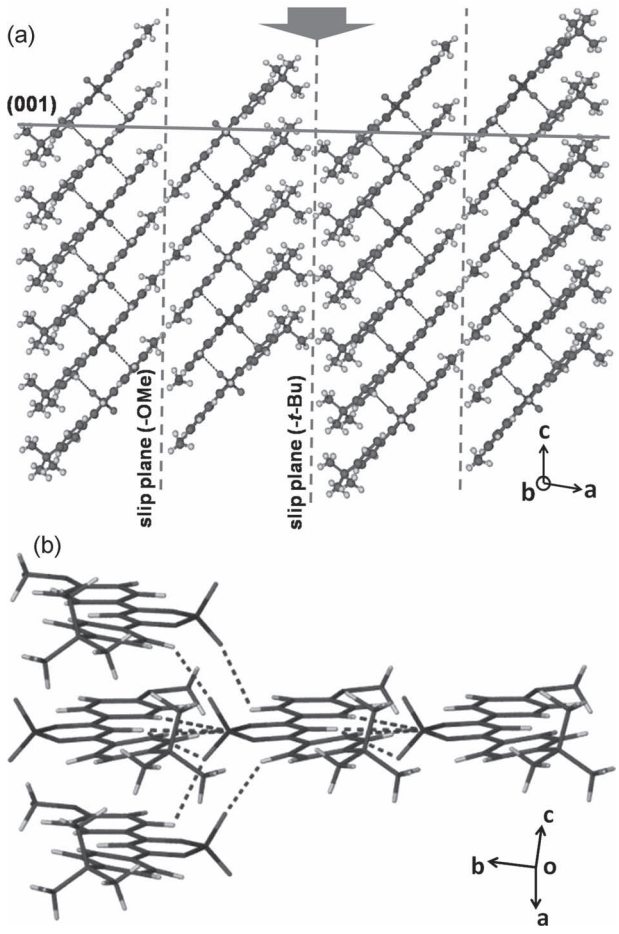

Figure 5. Crystal packing in cyan form II of BF_2AVB. a) Thick molecular sheets (between two slip planes) formed via multiple C–H···F interactions. Arrow indicates the indentation direction, i.e., perpendicular to (001) plane. b) Antiparallel stacking and multiple C–H···F interactions between molecules that form the thick 2D sheet.

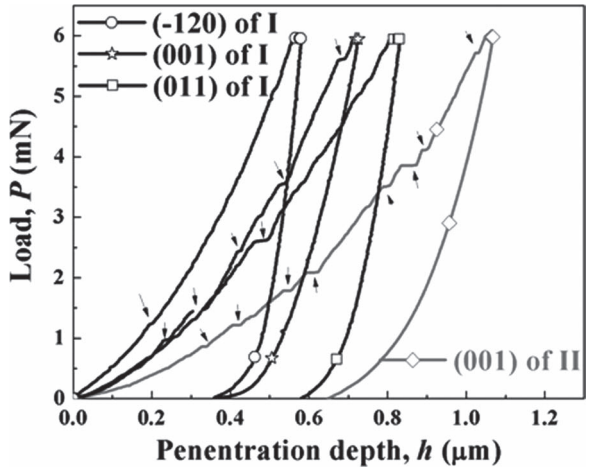

Figure 6. Representative *P-h* curves of BF_2AVB green polymorph (form I) crystals obtained with indentation normal to (011), (001) and (–120) planes. Also, *P-h* curve obtained on the (001) plane of the BF_2AVB cyan polymorph (form II) is shown. Arrows indicate discrete displacement bursts or pop-ins.

Table 1. Mechanical properties of BF_2AVB crystals obtained using nanoindentation with a Berkovich tip.

Polymorph	Orientation	Elastic Modulus, *E* [GPa]	Hardness, *H*[a)] [MPa]
Green/Form I (brittle, orthorhombic)	(011)	10.6 ± 0.35	275 ± 12
	(001)	7.4 ± 0.31	340 ± 7
	(–120)	13.2 ± 0.16	410 ± 11
Cyan/Form II (bending, monoclinic)	(001)	5.6 ± 0.46	206 ± 13

[a)]The error bars correspond to the standard deviations on the ten measurements that were made on each face.

only similarity between the major faces of both the polymorphs is that they are fracture resistant.

The average values of *E* and *H* extracted from the *P-h* curves using the standard methods are listed in **Table 1**. It shows that both *E* and *H* of form II are lower than any face of form I. This confirms the fact that form II is more compliant and softer than form I, in good agreement with the results of the qualitative mechanical tests that indicate form I is brittle whereas form II is ductile.

The atomic force microscopy (AFM) images of residual indent impressions obtained from all three faces of form I are shown in **Figure 7**. While no pile-up and/or fracture is seen along the (001) face, a small crack (indicated by arrow) is observed on one side of the indent corner for (011). In the case of (–120), significant pile-up along one side of the indent and several corner and radial cracks were observed. As the (–120) plane is at an oblique angle (≈22°) to the stack of 2D layers along (010), the pile-up is seen only on one side of the indenter faces. The pile-up during indentation occurs due to the volume conserving plastic deformation underneath the indenter.

2.3. Structure-Mechanical Property Correlations

To understand the connection between the underlying molecular structure and the measured mechanical properties, the crystal packing along each indentation direction on different faces needs to be considered. We first discuss the plastic properties of brittle form I. Among the three orientations studied, (–120) is found to be the hardest and (011) is the softest. As the molecular layers make a small oblique angle (≈12°) with the (–120) face, the indentation on this face is nearly perpendicular to the molecular layers (Figure 4c). Since there are no potential slip planes parallel to this direction, higher hardness is obtained. The packing perpendicular to (011) is also similar to that of the (–120) face, but at an oblique angle (22°) with the plane of the 2D layers (Figure 4b). Consequently, this angle results in the lowest *H* values on this plane. The extent of slip in various orientations depends on the magnitude of the shearing stress produced by the load applied and its orientation with respect to the active slip planes. Slip begins when the shearing stress on this slip plane, in the slip direction, reaches a threshold value, which is referred to as the critical resolved shear stress (CRSS).

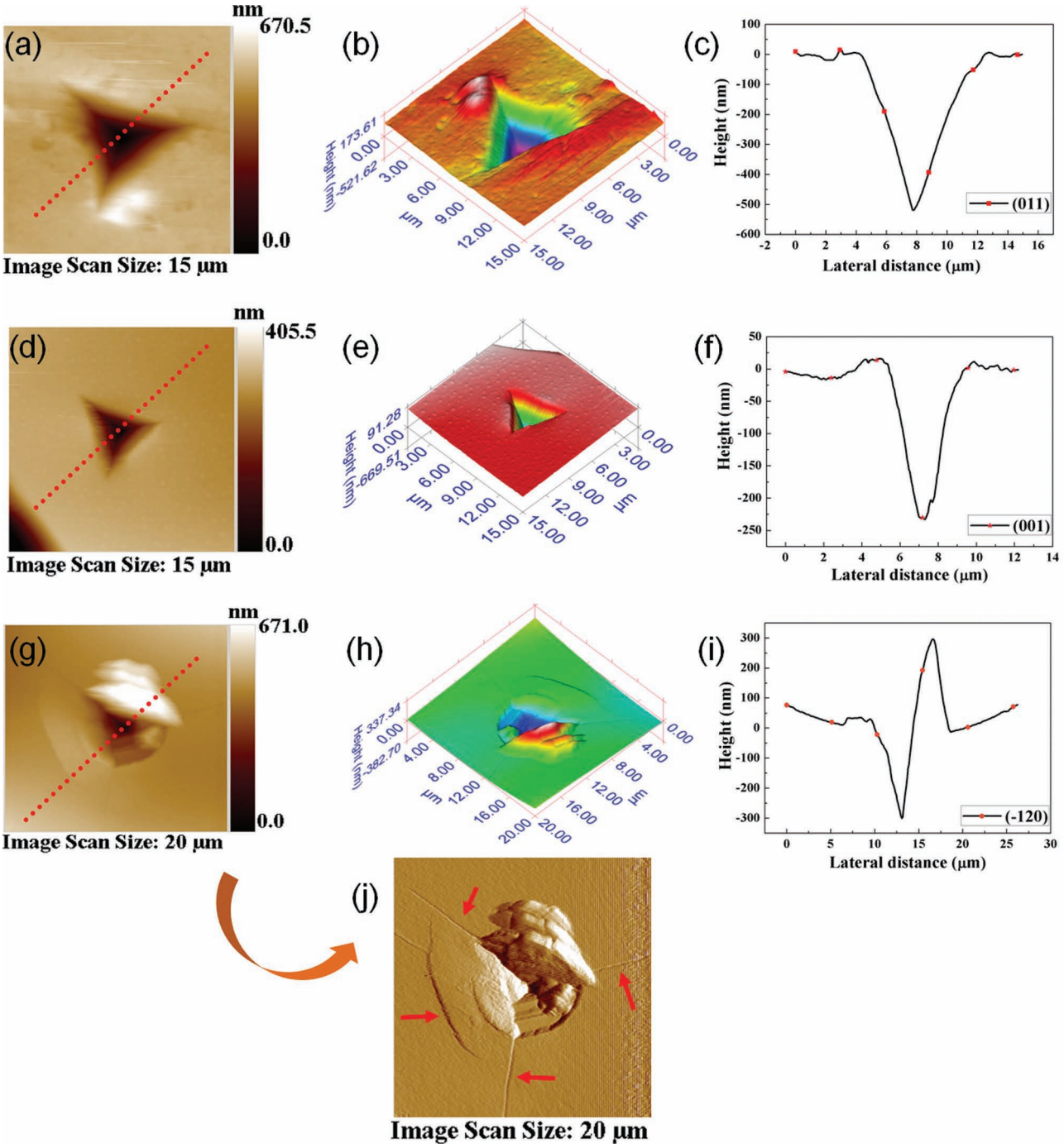

Figure 7. The AFM images, 3D representation and their corresponding line profiles at the middle of the residual indent impressions of a–c) (011), d–f) (001) and g–i) (–120) facets of form **I**. j) The phase AFM image of (–120) for form I shows significant cracks along the corners and radial cracks in the vicinity of the Berkovich indenter. The red dotted lines on the 2D AFM scans represent the positions where the line profiles were drawn.

CRSS is maximum when the angle between the normal to the slip plane and the compression axis, ϕ, and the angle which the slip direction makes with the compression axis, λ, are both 45° as CRSS is directly proportional to the product cos ϕ cos λ.[12] This product is known as the Schmid factor, m. Thus, if the compression axis is normal to the slip plane ($\lambda = 90°$) or if it is parallel to the slip plane ($\phi = 90°$), $m = 0$ and slip will not occur in these orientations. Crystals with these orientations tend to fracture rather than slip. From the Schmid's law,[12] the primary slip system will be the system with the greatest m. Calculated values of m and corresponding hardness values are given in **Table 2** (Figure S1, Supporting Information).

Table 2. Schmid factors of various slip systems for different planes of BF_2AVB form I crystals.

Plane	(011)	(001)	(–120)
Indentation direction	[0–16]	[001]	[810]
Slip plane	(010)	(010)	(010)
Slip direction	[001]	[001]	[100]
Schmid factor, *m*	0.48	0.35	0.24
Hardness [MPa]	275 ± 12	340 ± 7	410 ± 11
2D layers arranged (°) with respect to indentation plane	22	90	12

The molecular layer arrangement with respect to the (–120) plane is at an angle of ca. 12°, and the indenter axis is close to normal to the slip plane, *m* is relatively smaller, therefore severe fracture is seen rather than slip. As the applied load is perpendicular to the layers, the inter-layer distance is expected to decrease first (due to elastic compression). But, as they come closer, when the resistance offered by them or the elastic strain energy exceeds a critical fracture energy, cracking ensues. This is the reason for the observation of radial or corner cracks during the indentation on (–120). These cracking events manifest as pop-ins or displacement bursts in the *P-h* curves.

Next we turn our attention to elastic anisotropy and its correlation with the underlying crystal packing. As shown in the Table 1, the elastic modulus of the (–120) face is found to be the highest, whereas it is lowest for (001). In the case of indentation on the (001) face, the indenter passes parallel to the molecular layers (Figure 4c), i.e., perpendicular to the weak π-stacking interactions, which contribute little to the elastic recovery. This results in the lowest *E* on this face. In the case of (011), as the indentation direction is ≈ 60° to the layers, the elastic recovery is contributed by both interactions that govern the layer formation and the π-stacking interactions that recover on release of compressive force.[13] Hence, its *E* is slightly higher than that of the (001) face.

The crystal packing in form II (Figure 5a) suggests that the two major slip planes (*tert*-Bu and -OMe groups) are parallel to the indentation direction, i.e., perpendicular to the (001). The intermolecular interactions across the slip planes in form II are much weaker than that present in form I. Hence, as expected, *H* and *E* of (001) of form II are much lower than that of any face of the form I crystals. This supports our analysis that the slip planes in form I are not as active as in form II.

The results of this work suggest that both the elastic and plastic deformations in different orientations of the crystals are connected to crystallographic features. Discrete plastic deformation during nanoindentation is extensively reported for various other materials.[14–16] In metallic and inorganic crystal systems with initially low dislocation densities, it occurs due to nucleation of dislocation loops or their rapid multiplication during the indentation[17] whereas in amorphous alloys it is due to nucleation of shear bands.[18] However, in organic crystals, plastic deformation is attributed to glide (or slip), twinning and kinking, all in simple shear.[19] Bandyopadhyay et al.[19] reported that plastic deformation is more likely due to twinning for crystals with low symmetry and few slip systems or when plastic deformation is hindered due to unfavourable alignment and under high loading rates. The primary slip plane in organic materials is assumed to be the weakest plane in that the attachment energy on this plane is the least (for instance, *tert*-Bu and –OMe slip planes in form II). However, Olusanmi et al.[20] have argued that the low attachment energy alone is not a sufficiently reliable indication of the cleavage plane, for example, in case of aspirin. While the predicted active slip plane in the BF_2AVB form I crystal is parallel to (010), it is (100) for form II.

2.4. Mechanochromic Luminescence (ML) Studies

Having examined the mechanical behavior of the polymorphs I and II, we turn our attention to evaluate 1) the earlier hypotheses that plastic deformation or disruption of crystal packing is responsible for the ML behavior in fluorescent molecular crystals and 2) the reasons for the reversible nature of the ML behavior in the BF_2AVB polymorphs. We examined the ML behavior in forms I (green) and II (cyan) by crushing their single crystals separately in a clean and dry mortar with a pestle. When this is done in a warm mortar (taken out from an oven at 60 °C), gentle crushing results in a thin layer of powder particles (this process did not result in any change in the emission colour for both the forms, probably because this did not result in a significant density of defects in the resulting particles; **Figures 8**a and **9**a). However, upon scratching firmly with a pestle, the powders of the brittle green form I, exhibited a slight color change, which was barely detectable (Figure 8b). Careful inspection revealed that the material indeed showed a color change from green to yellow upon grinding, but faded back quickly to green, along the path of pestle movement (resembling the fading tail of a satellite in the earth's atmosphere). At room temperature (rt), the change in emission color was more prominent, but not dramatically different. As the mechanical properties of molecular crystals depend upon temperature,[10] we repeated this at –98 °C (Figures 8d–f) by immersing the mortar into methanol followed by cooling using liquid nitrogen. The material showed a clear color change from green to yellow (Figure 8e) and took some minutes before recovering to the original green colour (Figure 8f). On the other hand, the cyan (bending) form II showed a prominent colour change to yellow (Figure 9b) upon scratching firmly even above room temperature (~ 55 °C), but it also healed back to cyan, slowly at 55 °C or more quickly by heating (Figure 9c).

The ML experiments reveal three things: 1) the perturbed yellow states, on recovery, emit the same colour as their parent forms do, 2) the ML behavior of form II is more prominent than in form I at a same temperature, and 3) the recovery in the green form I is faster than in the cyan form II. The latter observation indicates a clear relationship between the reversible mechanochromism and mechanical properties of the crystalline forms, i.e., the stiffer form recovers quickly from the metastable state to the original. For form I all three faces show higher elastic recovery rate prior to the onset of elastic-plastic transition (first pop-in in the *P-h* curve) than for form II, (Figure 6). The fact that the perturbed states recover to emit the initial colour, suggests that these states must remain close enough to

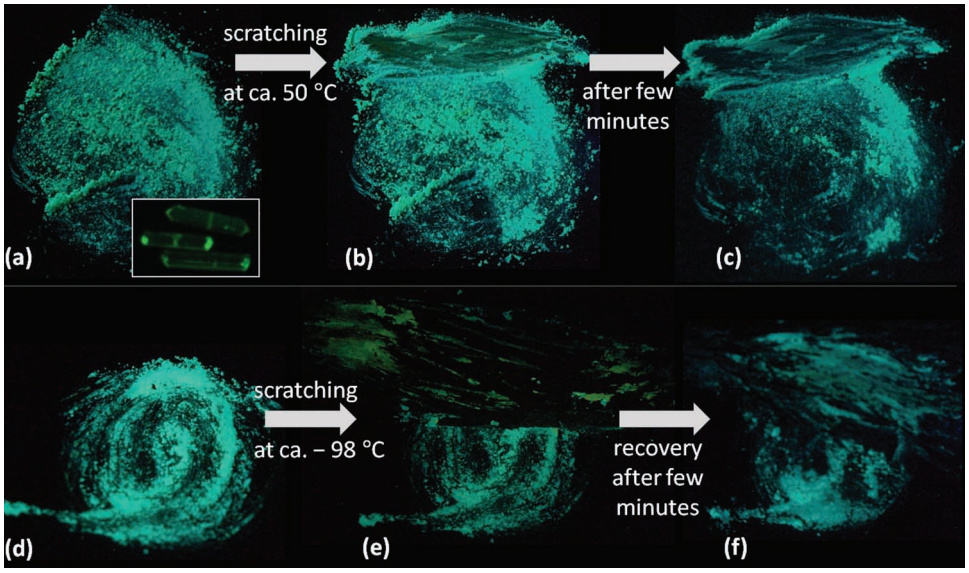

Figure 8. BF_2AVB green form I. a) Crystalline solid film obtained by crushing green crystals (inset) gently in a warm mortar at ca. 55 °C (dried at 60 °C in an oven). b) The film just after scratching shows a barely detectable color change to yellow (top). c) Film after heating with a hot-air gun for about a minute. The images in (d–f) correspond to the experiment repeated at a lower temperature of ca. –98 °C. Notice the prominence of color change to yellow in (e), compared to the higher temperature sample in (b), and recovery to parent color, green in (f).

the crystal structure of the initial form, but with defects that cause some changes in the molecular environment, so that they return to the original form over time or on heating. This means that the perturbed states do not convert to other stable solid-state forms, but only revert to the parent form.

To check if forms I and II can interconvert or transform to other form, we carried out mechanical grinding (dry) experiments extended for about 30 minutes. A quick visual inspection revealed that the powders appear more yellowish just after grinding. They do not convert to any other form, but with time or on heating recover to their parent forms: the stiffer form I recovers quickly to the original state compared to the softer form II, as indicated by powder X-ray diffraction (Figure S2,S3, Supporting Information). Differential scanning calorimetry (DSC) of as grown single crystals showed no phase transition endotherms before melting, confirming no detectable phase transition by thermal means (Figure S4, Supporting Information). Another favourable factor for reversible ML behavior may be that the original phase acts as a nucleating agent for the transformation of perturbed states back to the original state. These observations suggest that the solid-state packing in the perturbed state likely exists with some defects (e.g., misalignment of layers, π-stacking interactions or tilting of molecules in the layers) that are large enough to change the emitting wavelength, but energetically small enough to recover. Hence, as supported by the nanoindentation results, it is highly possible that the defects are formed mainly due to the breakage or rearrangement of weak interactions along the active slip planes, for example the π-stacking interactions in form I or the van der Waals interactions (*tert*-Bu, -OMe) in form II, rather than the breakage or disruption of stronger interactions. With external stimuli or with time, the material recovers back to the original form as moving molecules along these weak planes will not have high energy barriers.

3. Conclusion

Investigation of the mechanical properties of green and cyan BF_2AVB crystals using qualitative deformation tests and

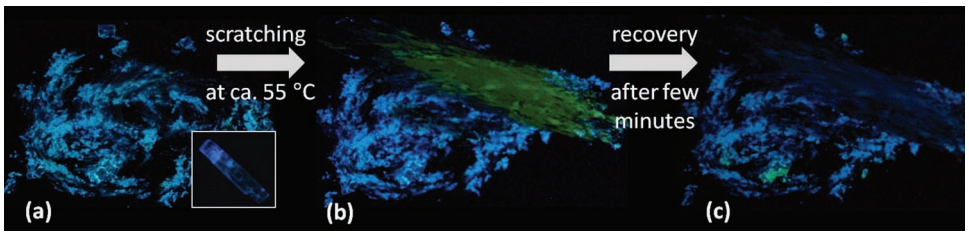

Figure 9. BF_2AVB cyan form II. a) Powder solid film obtained by crushing cyan crystals (inset) gently in a warm mortar at ca. 55 °C. b) The film just after scratching firmly shows bright color change to yellow (top-right). c) Film after heating with a hot-air gun for about a minute. Notice the prominent color change to yellow in (b) and recovery to the parent cyan in (c).

nanoindentation (quantitative) techniques confirm that the cyan form II is much softer and more compliant compared to the green form I. A detailed crystal structure analysis of the two forms suggests that the presence of slip planes in form II is responsible for its higher plasticity compared to form I which has a nearly isotropic structure, and hence is brittle. Indentation experiments confirmed that the hardness of form II is significantly less than any face of form I. From the crystal packing, it is clear that the structure of form II is more anisotropic than that of form I, given stronger (multiple C–H···F) and weaker interactions (*tert*-Bu, -OMe) in the former. The experimentally established structure-mechanical property relationship is in excellent agreement with the ML behavior of forms I and II. Although both form I and II show ML behavior, it is much more prominent in form II given a slower recovery rate, which we attribute to its greater plasticity. But with time or upon heating, the perturbed yellow emitting states of both forms recover to their parent polymorphic forms, as suggested by the emission colours of the healed solids. This implies that the perturbed states are metastable in nature and must remain close enough to the structure of the parent form to recover, but not transform to any other stable solid form. The findings do not seem consistent with phase changes to new solid state forms. Instead, we propose that the reversibility of the ML behavior is likely due to the presence of weak interaction (slip) planes with nonspecific van der Waals interactions that lead to recoverable defects. Associated shear induced or enabled molecular shape changes may also be occurring and cannot be ruled out. These observations with BF_2AVB polymorphs suggest that the introduction of active slip planes in solid-state structures of a fluorophore could be a valuable design strategy to enhance the ML behavior for practical applications.

These studies with BF_2AVB polymorphs advance molecular level understanding of the ML optical phenomenon in solid-state materials, which is significant as mechanistic understanding remains a challenge in the field. The dynamic ML aspects of the polymorphs also support the recent suggestions that molecules could experience large amplitude motions in the crystalline state, especially when energized by mechanical grinding[21] or light.[22] Our results with BF_2AVB support the view that the crystalline arrangement of molecules upon activation has to be considered as dynamic rather than static as determined from X-ray crystallography.[22]

4. Experimental Section

BF_2AVB was synthesized according to the previously reported procedure[7] and crystallized in acetone solution by slow evaporation at ambient conditions. From most batches, only the green form was obtained, but occasionally the cyan form was also found concomitantly. The two polymorphic forms were separated under UV (365 nm), based on their emission colours. The selected crystals of form I and form II were firmly mounted on a stud using a thin layer of cyanoacrylate glue prior to nanoindentation. Indentation experiments were possible on (011), (001) and (–120) of I and the (001) of II faces using a nanoindenter (Triboindenter of Hysitron, Minneapolis, USA) with an in situ imaging capability. The machine continuously monitors and records the load, *P*, and displacement, *h*, of the indenter with force and displacement resolutions of 1 nN and 0.2 nm, respectively. A three-sided pyramidal Berkovich diamond indenter (tip radius ≈100 nm) was used to indent the crystals. Loading and unloading rates of 0.6 mN/s and a hold time of 30 s at peak load were employed. In order to identify flat regions for the experiment, the crystal surfaces were imaged prior to indentation using the same indenter tip. A minimum of 10 indentations were performed on each crystallographic face to ensure reproducibility. The indentation impressions were captured immediately after unloading so as to avoid any time-dependent elastic recovery of the residual impression. The *P-h* curves obtained were analyzed using the standard Oliver-Pharr method[17,23] to extract the elastic modulus, *E*, of the crystal in that orientation.

Acknowledgements

G.R.K. thanks IISER Kolkata for SRF. M.S.R.N.K. thanks the University Grants Commission, Govt. of India for a Dr. D. S. Kothari Post-Doctoral Fellowship. C.M.R. acknowledges financial support from the DST (SR/FT/CS-074/2009). C.L.F. thanks the US National Science Foundation for support (CHE 0718879; CHE 1213915).

Received: July 9, 2012
Published online: October 16, 2012

[1] a) R. H. Friend, R. W. Gymer, A. B. Holmes, J. H. Burroughes, R. N. Marks, *Nature* **1999**, *397*, 121; b) C. A. Strassert, C. Chien, M. D. G. Lopez, D. Kourkoulos, D. Hertel, K. Meerholz, L. De Cola, *Angew. Chem. Int. Ed.* **2011**, *50*, 946.

[2] a) J. Schmidtke, W. Stille, H. Finkelmann, S. T. Kim, *Adv. Mater.* **2002**, *14*, 746; b) F. Gao, Q. Liao, Z. Xu, Y. Yue, Q. Wang, H. Zhang, H. Fu, *Angew. Chem. Int. Ed.* **2010**, *49*, 732.

[3] W. Denk, *Proc. Natl. Acad. Sci. USA* **1994**, *91*, 6629.

[4] S. J. Yoon, J. W. Chung, J. Gierschner, K. S. Kim, M. G. Choi, D. Kim, S. Y. Park, *J. Am. Chem. Soc.* **2010**, *132*, 13675.

[5] H. Ito, T. Saito, N. Oshima, N. Kitamura, S. Ishizaka, Y. Hinatsu, M. Wakeshima, M. Kato, K. Tsuge, M. Sawamura, *J. Am. Chem. Soc.* **2008**, *130*, 10044.

[6] D. Yan, A. Delori, G. O. Lloyd, T. Friščić, G. M. Day, W. Jones, J. Lu, M. Wei, D. G. Evans, X. Duan, *Angew. Chem. Int. Ed.* **2011**, *50*, 12483.

[7] G. Zhang, J. Lu, M. Sabat, C. L. Fraser, *J. Am. Chem. Soc.* **2010**, *132*, 2160.

[8] a) M. S. R. N. Kiran, S. Varughese, U. Ramamurty, G. R. Desiraju, *CrystEngComm* **2012**, *14*, 2489; b) M. S. R. N. Kiran, S. Varughese, C. M. Reddy, U. Ramamurty, G. R. Desiraju, *Cryst. Growth Des.* **2010**, *10*, 4650; c) K. J. Ramos, D. E. Hooks, D. F. Bahr, *Philos. Mag.* **2009**, *89*, 2381; d) J. C. Tan, J. D. Furman, A. K. Cheetham, *J. Am. Chem. Soc.* **2009**, *131*, 14252; e) J. C. Tan, A. K. Cheetham, *Chem. Soc. Rev.* **2011**, *40*, 1059.

[9] S. Varughese, M. S. R. N. Kiran, K. A. Solanko, A. D. Bond, U. Ramamurty, G. R. Desiraju, *Chem. Sci.* **2011**, *2*, 2236.

[10] a) C. M. Reddy, R. C. Gundakaram, S. Basavoju, M. T. Kirchner, K. A. Padmanabhan, G. R. Desiraju, *Chem. Commun.* **2005**, 3945; b) C. M. Reddy, M. T. Kirchner, R. C. Gundakaram, K. A. Padmanabhan, G. R. Desiraju, *Chem. Eur. J.* **2006**, *12*, 2222; c) C. M. Reddy, K. A. Padmanabhan, G. R. Desiraju, *Cryst. Growth Des.* **2006**, *6*, 2720; d) C. M. Reddy, G. R. Krishna, S. Ghosh, *CrystEngComm* **2010**, *12*, 2296.

[11] a) P. Panini, D. Chopra, *CrystEngComm* **2012**, *14*, 1972; b) K. Reichenbächer, H. I.Süss, J. Hulliger, *Chem. Soc. Rev.* **2005**, *34*, 22.

[12] E. Schmid, *Z. Elektrochem.* **1931**, *37*, 447.

[13] a) G. M. Espallargas, L. Brammer, D. R. Allan, C. R. Pulham, N. Robertson, J. E. Warren, *J. Am. Chem. Soc.* **2008**, *130*, 9058; b) E. V. Boldyreva, *J. Mol. Struct.* **2003**, *647*, 159; c) H. N. Bordallo,

E. V. Boldyreva, A. Buchsteiner, M. M. Koza, S. Landsgesell, *J. Phys. Chem. B* **2008**, *112*, 8748.
[14] D. Casellas, J. Caro, S. Kolas, J. M. Prado, I. Valls, *Acta Mater.* **2007**, *55*, 4277.
[15] C. A. Schuh, J. K. Mason, A. C. Lund, *Nat. Mater.* **2005**, *4*, 617.
[16] D. F. Bahr, D. E. Kramer, W. W. Gerberich, *Acta Mater.* **1998**, *46*, 3605.
[17] W. C. Oliver, G. M. Pharr, *J. Mater. Res.* **1992**, *7*, 1564.
[18] a) P. Murali, U. Ramamurty, *Acta Mater.* **2005**, *53*, 1467; b) B. Viswanath, R. Raghavan, U. Ramamurty, N. Ravishankar, *Scripta Mater.* **2007**, *57*, 361; c) N. Gane, *Proc. R. Soc. London A* **1970**, *317*, 367; d) S. Sridhar, A. E. Giannakopulous, S. Suresh, U. Ramamurty, *J. Appl. Phys.* **1999**, *85*, 380.
[19] R. Bandhopadhyay, D. J. S. Grant, *Pharm. Res.* **2002**, *19*, 491.
[20] D. Olusanmi, K. J. Roberts, M. Ghadiri, Y. Ding, *Int. J. Pharm.* **2011**, *411*, 49.
[21] A. V. Trask, N. Shan, W. D. S. Motherwell, W. Jones, S. Feng, R. B. H. Tan, K. J. Carpenter, *Chem. Commun.* **2005**, 880.
[22] B. R. Bhogala, B. Captain, A. Parthasarathy, V. Ramamurthy, *J. Am. Chem. Soc.* **2010**, *132*, 13434.
[23] A. Bolshakov, W. C. Oliver, G. M. Pharr, *J. Mater. Res.* **1996**, *11*, 760.